



HAL
open science

What is the influence of two strain rates on the relationship between human cortical bone toughness and micro-structure?

Rémy Gauthier, Hélène Follet, Max Langer, Françoise Peyrin, David Mitton

► To cite this version:

Rémy Gauthier, Hélène Follet, Max Langer, Françoise Peyrin, David Mitton. What is the influence of two strain rates on the relationship between human cortical bone toughness and micro-structure?. Proceedings of the Institution of Mechanical Engineers, Part H: Journal of Engineering in Medicine, 2020, 234 (3), 16 p. 10.1177/0954411919884776 . hal-02441823

HAL Id: hal-02441823

<https://hal.science/hal-02441823>

Submitted on 16 Jan 2020

HAL is a multi-disciplinary open access archive for the deposit and dissemination of scientific research documents, whether they are published or not. The documents may come from teaching and research institutions in France or abroad, or from public or private research centers.

L'archive ouverte pluridisciplinaire **HAL**, est destinée au dépôt et à la diffusion de documents scientifiques de niveau recherche, publiés ou non, émanant des établissements d'enseignement et de recherche français ou étrangers, des laboratoires publics ou privés.

What is the influence of two strain rates on the relationship between human cortical bone toughness and micro-structure?

Rémy Gauthier^{1,2}, Hélène Follet³, Max Langer², Françoise Peyrin^{2,4} and David Mitton^{1,*}

¹Univ Lyon, Université Claude Bernard Lyon 1, IFSTTAR, LBMC UMR_T9406, F69622, Lyon, France ;

²Univ Lyon, CNRS UMR 5220, Inserm U1206, INSA Lyon, Université Claude Bernard Lyon 1, Creatis, F69621 Villeurbanne, France ;

³Univ Lyon, Université Claude Bernard Lyon 1, INSERM, LYOS UMR1033, F69008, Lyon, France ;

⁴ESRF, 38, Grenoble France.

* david.mitton@ifsttar.fr

Abstract: Cortical bone fracture mechanisms are well studied under quasi-static loading. The influence of strain rate on crack propagation mechanisms needs to be better understood, however. We have previously shown that several aspects of the bone micro-structure is involved in crack propagation, such as the complete porosity network, including the Haversian system and the lacunar network, as well as biochemical aspects, such as the maturity of collagen cross-links. The aim of this study is to investigate the influence of strain rate on the toughness of human cortical bone with respect to its microstructure and organic non-collagenous composition. Two strain rates will be considered: quasi-static loading (10^{-4} s^{-1} , a standard condition, and a higher loading rate (10^{-1} s^{-1}), representative of a fall. Cortical bone samples were extracted from 8 female donors (50 y.o. to 91 y.o.). Three- point bending tests were performed until failure. Synchrotron radiation micro-computed tomography imaging was performed to assess bone microstructure including the Haversian system and the lacunar system. Collagen enzymatic cross-link maturation was measured using a high performance liquid chromatography column. Results showed that that under quasi-static loading, the elastic contribution of the fracture process is correlated to both the collagen cross-links maturation and the microstructure, while the plastic contribution is correlated only to the porosity network. Under fall-like loading, bone organization appears to be less linked to crack propagation.

Keyword: Human cortical bone, crack propagation, synchrotron micro-computed tomography, Haversian canals, osteocytes lacunae, collagen cross-links, paired anatomical locations

Introduction

From a clinical point of view, the prediction of bone fracture risk remains difficult while more than 9 million fractures occur every year¹⁻³. Clinical gold standard methods are still relying on the assessment of bone mineral density (BMD) using Dual-energy X-ray Absorptiometry (DXA)⁴.

BMD is however not sufficient to accurately predict the fracture risk^{1,2}. Even if BMD is a good predictor of bone strength⁵, this single parameter does not describe the overall mechanical response of bone in a fall loading configuration⁶. Other parameters, related to the geometry, the material composition or the architecture of bone, have to be considered to understand the bone fracture process^{7,8}.

Toughness appears to be one relevant biomechanical parameter to understand bone fracture mechanisms⁹. During crack propagation, a number of toughening mechanisms occur in order to slow and stop the crack during its propagation and thus increase the energy needed to break the material¹⁰⁻¹⁴. These mechanisms depend on the structural organization of the bone tissue: micro-crack formation is associated to the Haversian network¹⁵, cracks are deflected along the long axis of the osteons following the cement lines^{16,17} and interfibrillar sliding might be associated to the maturity of the collagen^{18,19}.

These so called toughening mechanisms have been widely studied under standard quasi-static loading, but there are only few data considering higher loading rates²⁰⁻²². This despite fractures mainly occurring after falls from a standing position²³. We recently showed that cortical bone toughness in different anatomical locations is significantly decreased at a higher strain rate compared to a standard quasi-static loading²⁴. In order to better understand the bone fracture process in the case of a fall, the influence of microstructure and biochemical composition on the decrease in toughness should be studied.

The aim of this study is thus to investigate relationships between the bone toughness and its structural and compositional properties both under quasi-static and fall-like loading conditions in order to provide new insight regarding cortical bone crack propagation mechanisms. The current study builds on previous results on human cortical bone toughness²⁴, microstructure²⁵ and collagen cross-link composition²⁶.

Materials and methods

Bone samples

The investigations were performed on 8 paired femoral diaphyses, femoral necks and radial diaphyses extracted from female donors (average: 70 y.o, min: 50 y.o., max: 91 y.o.). No medical history of the donors was available. After extraction, the bones were kept hydrated within gauze soaked with saline and stored at $-20\text{ }^{\circ}\text{C}$ until sample preparation.

Biomechanical measurements

The biomechanical experiments were performed following the experiment protocol used in ²⁴. Two contiguous rectangular specimens from each bone, between 20 and 25 mm long, 2.1 ± 0.1 mm width and 1.0 ± 0.1 mm thick, their long axis parallel to the main axis of the bone, were prepared using a low speed saw with a diamond coated blade (ISOMET 4000, Buehler, USA). They were then notched in their middle perpendicularly to the long axis of the diaphysis and subjected to a three point bending test until failure (Figure 1). Each contiguous sample was submitted either to standard quasi-static loading (10^{-4} s^{-1}) or fall-like loading (10^{-1} s^{-1} , ²⁷) to assess the influence of the loading rate. Samples were re-hydrated in saline solution 24 h before the mechanical tests. Toughness parameters were then investigated using the ASTM E-1820 ²⁸. The details can be found in ²⁴.

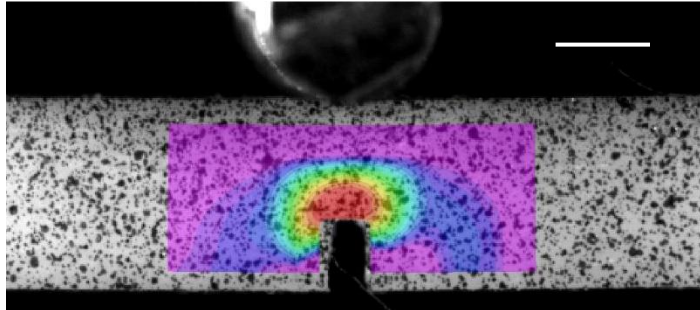


Figure 1 Cortical SENB sample under a critical loading following the ASTM E-1820. Strain field is calculated using Digital Image Correlation (Vic-2D, Correlated Solutions, Columbia, USA). Red color represents the highest value of strain. Note the strain concentration around the notch. Scale bar: 1mm.

The parameters assessed in the current study are the elastic contribution to toughness J_{el} ($\text{kN}\cdot\text{m}^{-1}$), the plastic contribution J_{pl} ($\text{kN}\cdot\text{m}^{-1}$), and the global toughness parameter $J = J_{el} + J_{pl}$ ($\text{kN}\cdot\text{m}^{-1}$). They give the energy needed to initiate (J_{el}) and propagate (J_{pl}) a crack through bone structure ²⁴. These parameters are called the energy release rates, and are closely related to the toughness ²⁹. For the sake of simplicity, we will use the term toughness when referring to these parameters.

Synchrotron Radiation micro-Computed Tomography (SR- μ CT)

After the biomechanical experiments, Synchrotron Radiation micro-Computed Tomography (SR- μ CT) imaging was used to assess cortical bone microstructure from the Haversian system down to the lacunar system in the samples²⁵. The scanned region of interest was chosen outside the rollers of the mechanical set up so as to not be affected by the mechanical loading. The fractured samples were delipidated one week before imaging: the samples were immersed in acetone for 30 minutes, then rinsed with water, and finally dehydrated by successive immersion in 70 % and nearly 100 % ethanol baths for a maximum period of 2 days. Image acquisition was performed on beamline ID19 at the European Synchrotron Radiation Facility (ESRF, Grenoble, France) using a “pink beam” filtered undulator radiation with an effective energy of 31 keV. Volumes of 2048^3 voxels with a nominal voxel size of $0.7\mu\text{m}$ were finally obtained from each sample.

In the current study, we mainly consider the following structure parameters: the Haversian canal diameter (On.Ca.Dm, in μm), the lacunar density (Lc.N/BV, in mm^{-3}) and the average lacunar radius of curvature (Lc. ρ_1 , in μm) defined as:

$$Lc.\rho_1 = \frac{(Lc.L_2)^2}{Lc.L_1},$$

where Lc.L₁ (μm) and Lc.L₂ (μm) are the dimensions of the first and second axis of an ellipsoid fitted to the lacuna, respectively³⁰.

Biochemical measurements

The collagen cross-links were measured using a high performance liquid chromatography column as done in²⁶. These measurements were performed on bone tissue that remained from the preparation of samples for the mechanical tests, i.e. tissue adjacent to these samples in the bone. In the current study, we focused on the CX ratio which is the ratio between divalent (immature) and trivalent (mature) enzymatic cross-links. This parameter reflects the maturation of the collagen matrix: a more mature collagen matrix implies a lower CX ratio.

Statistical tests

In order to make statistical tests on more than 8 samples, a longitudinal study was performed by pooling the three anatomical locations to finally have a population of 24 samples for each biomechanical, microstructural or biochemical parameter (8 femoral diaphyses, 8 femoral necks and 8 radial diaphyses). Analyses were also performed for each individual site to have information on their respective contributions.

Shapiro-Wilk’s normality tests were not satisfied for some of the parameters. Therefore, Spearman’s rank correlation coefficient was used to investigate correlations between the measured parameters.

Multiple linear regressions using backward stepwise elimination to remove the non-significant parameters were performed until obtaining significant relation to explain the variance of the biomechanical parameters. Statistical significances were considered at $p < 0.05$. The statistical analysis was performed using StatView (StatView, Abaqus, USA).

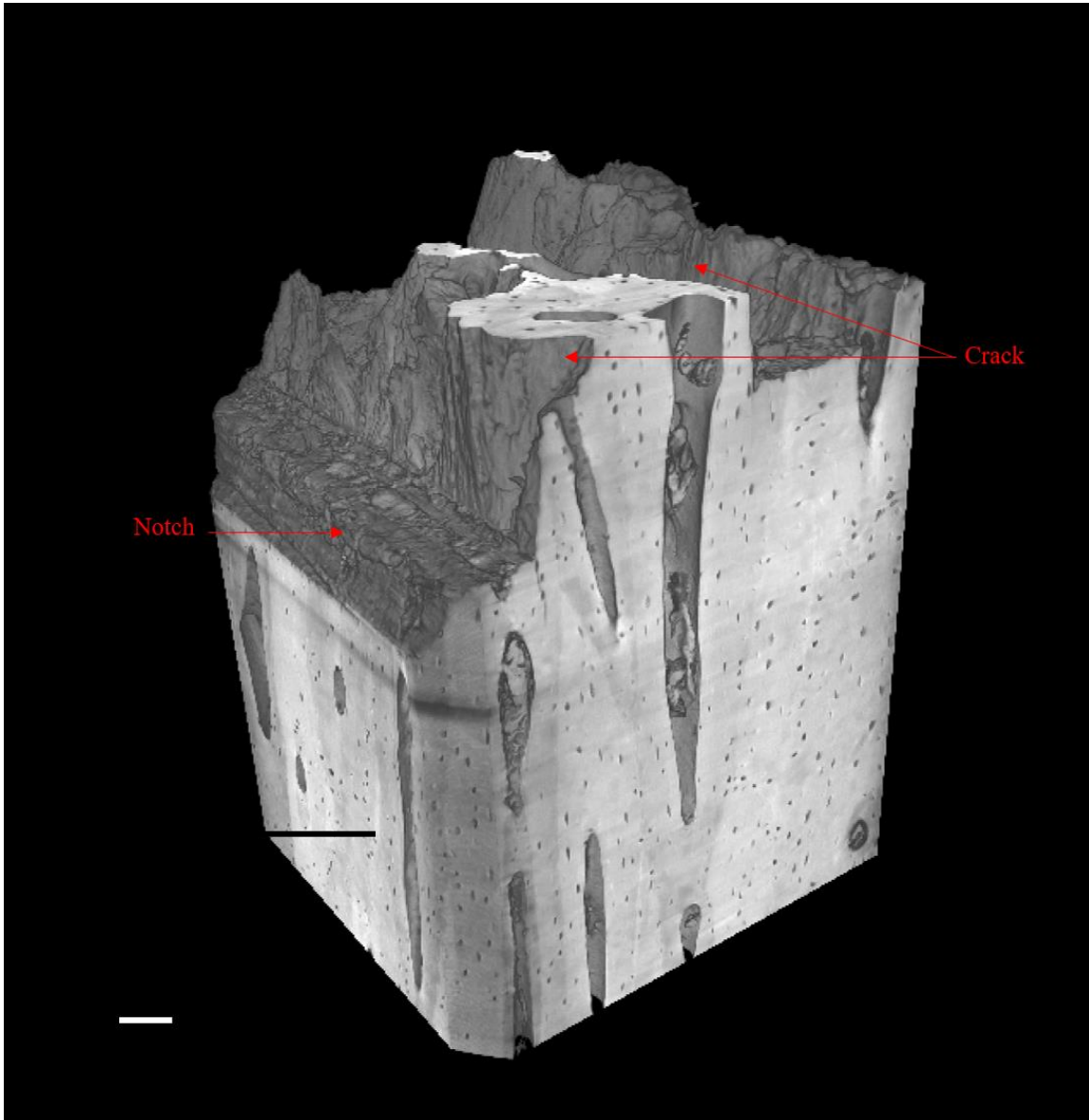


Figure 2 Volume rendering of a radial diaphysis sample after subjected to critical loading (woman, 73 y.o., scale bar = 500 μm)

Results

Figure 2 illustrates a volume rendering of one radius sample imaged after critical loading. On this 3D display, we can observe the Haversian canals appearing as the long

longitudinal porosities and the osteocyte lacunae as small porosities. Table 1 presents the Spearman's coefficients between biomechanical and structural or biochemical features. The detailed correlation for each anatomical location is shown on the table S1, S2 and S3 of the supplementary materials.

We first consider each location separately (Table S1, S2 and S3 in supplementary materials).

In the femoral diaphysis, under quasi-static loading J_{pl} and J is negatively correlated to lacunar density. Under fall-like loading, J_{el} is positively correlated with the CX ratio, and J_{pl} and J are negatively correlated to $Lc.N/BV$ (Table S1).

In the femoral neck, under quasi-static loading no significant correlations were found. Under fall-like conditions, however, J_{pl} is positively correlated to the CX ratio and negatively correlated to $Lc.\rho_1$ whereas J is negatively correlated to $Lc.\rho_1$ (Table S2).

In the radial diaphysis, no significant correlation was found for neither of the two loading conditions (Table S3).

We now consider the study over the 24 pooled samples (Table 1). Under quasi-static loading, J_{el} and J_{pl} as well as J were negatively correlated with $Ca.Dm$. All three toughness parameters J_{el} , J_{pl} , and J were positively correlated with $Lc.\rho_1$. J_{pl} , related to crack propagation, in particular showed a relatively strong correlation. Under fall-like loading conditions, J_{el} is negatively correlated to $Ca.Dm$ (Table 1). Table S4 (supplementary materials) presents similar results as Table 1 with more biochemical and structural parameters.

Table 1: Spearman's coefficient between the biomechanical, biochemical and structural parameters.

Biomechanical parameter	Rate	On. $Ca.Dm$	$Lc.N/BV$	$Lc.\rho_1$	CX
J_{el}	QS	- 0.42*	- 0.27	- 0.51*	- 0.18
	F	- 0.42*	- 0.19	- 0.17	0.21
J_{pl}	QS	- 0.45*	- 0.13	- 0.62**	0.05
	F	0.04	- 0.09	0.04	0.31
J	QS	- 0.45*	- 0.14	- 0.66**	0.06
	F	- 0.07	- 0.15	- 0.13	0.28

* $p < 0.05$; ** $p < 0.01$

Table 2 presents the best multivariate linear regression explaining biomechanical variances with structural and biochemical parameters, even considering all the biochemical and structural parameters presented in Table S4.

Multiple linear regression revealed several significant relations. Under quasi-static loading, for the elastic and plastic contribution of the toughness, the combination of On.Ca.Dm, Lc.N/BV and Lc. ρ_1 explains the variance in J_{el} up to 32 %, and the combination of the CX ratio, On.Ca.Dm and Lc. ρ_1 explains the variance of J_{pl} and J up to 50 % and 51 %, respectively.

Under fall-like loading, the combination of On.Ca.Dm, the CX ratio and Lc.N/BV explains the variance in J_{el} up to 39 %.

Table 2: Multivariate linear regression explaining the variance of biomechanical parameters.

	Best combination	p-value	Adj-R ²
J_{el}	QS $1.57 - 0.002 \times \text{On. Ca. Dm} - 2.16 \cdot 10^{-5} \times \text{Lc. } \frac{N}{BV} - 0.08 \times \text{Lc. } \rho_1$	0.02	0.32
	F $2.49 - 0.01 \times \text{On. Ca. Dm} - 7.68 \cdot 10^{-5} \times \text{Lc. } \frac{N}{BV} + 0.29 \times CX$	0.007	0.39
J_{pl}	QS $30.00 - 0.11 \times \text{On. Ca. Dm} - 2.90 \times \text{Lc. } \rho_1 + 2.39 \times CX$	0.007	0.50
	F -	-	-
J	QS $31.11 - 0.11 \times \text{On. Ca. Dm} - 2.99 \times \text{Lc. } \rho_1 + 2.39 \times CX$	0.001	0.51
	F -	-	-

QS: quasi-static ; F: fall

Figure 3 shows the estimate of J using the best combinations shown in table 2 as a function of the real measure of J.

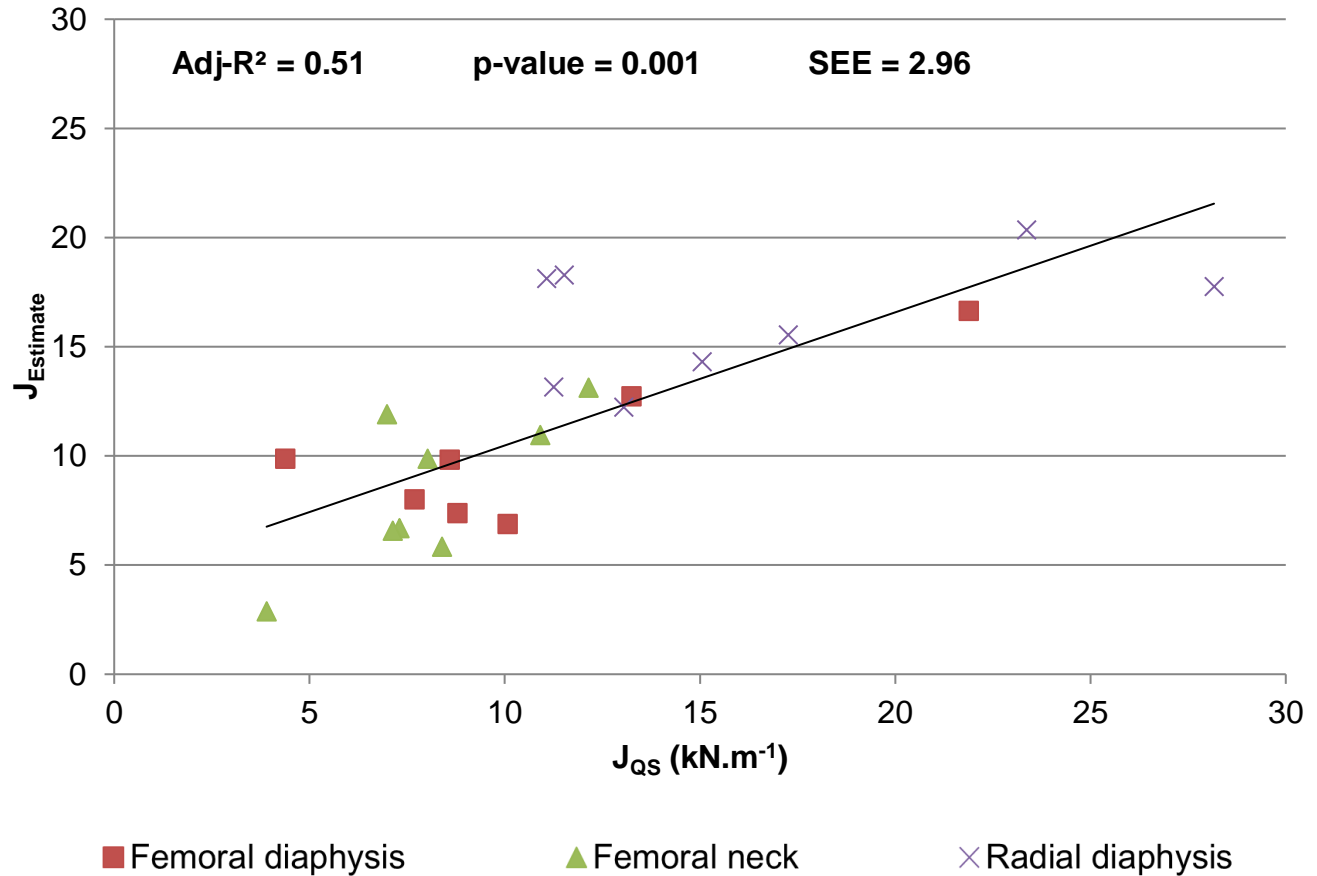


Figure 3: J_{QS} measured in function of J_{Estimate} using the equation in Table 2 (SEE = Standard Error of the Estimate).

Discussion

A better knowledge of human cortical bone crack propagation mechanisms is of great interest for a better care of bone fracture risk. Cortical bone is a complex material showing a multi-scale arrangement of organic and mineral³¹. In this study performed on 8 paired human femoral diaphyses, femoral necks and radial diaphyses, we investigated the influence on human cortical bone toughness of the Haversian system, the lacunar system, and the collagen matrix maturation at two loading conditions. The use of different anatomical locations allows the investigation of crack propagation mechanisms over a wide range of mechanical or organizational properties. To our knowledge, this is the first study to investigate human cortical bone toughness involving structural and compositional features at different length scales and considering two loading conditions.

Considering the elastic regime, we can observe that both the canal diameter and lacunar radius of curvature are correlated with the elastic toughness under quasi-static loading. Significant correlations between the elastic toughness and the Haversian system have already been found in the past³²⁻³⁴. A significant decrease of the yield stress with the

increase of the canal diameter has also been observed³⁵. These results are in agreement with our results. The initiation of the crack is governed by the stretching of the tissue in the neighborhood of the notch, thus involving the stretching of mineralized collagen molecules³⁶. It has been shown that the elastic behavior at the tissue level is associated with the behavior at the fibrillar or mineral scale³⁷. It is also known that the Haversian canal parameters are correlated with bone elastic properties³⁸⁻⁴⁰, which is confirmed here as we find a significant correlation between canal diameter and elastic toughness. A relationship between the initiation toughness and the lacunar system has also previously been observed³³. There is fewer data available at this scale, however.

The hypothesis is here that lacunae may play a role of stress concentrators⁴¹⁻⁴⁴. It is known from the field of fracture mechanics that small defects have the capacity to concentrate stresses during the loading^{45,46}. This means that the stress around these defects is higher than in the surrounding environment (see on Figure 1 the strain concentration around the notch). It has been shown that the strain in the neighborhood of lacunae was increased relative to the surrounding tissue^{41,43,47}. By playing the role of such defects, the lacunae can concentrate some stresses during the loading, and thus relax the notch. Actually, for a same mechanical energy provided to the material, if the notch is placed in an homogeneous medium, all the energy will be concentrated around it ; nevertheless if other small defects surround this notch, some of the total energy will be used to concentrate the stress around these small defects, thus the stress concentration state around the notch will be lowered This will increase the energy needed to initiate a crack from the notch. Furthermore, a stress concentrator with a smaller radius of curvature will concentrate even more stress⁴⁶, which supports the negative correlation we found here. Regarding the multiple linear regression, we can observe that the lacunar density help to better estimate the elastic toughness. This suggests that when cortical bone has a lower density of lacunae, it can better resist crack propagation. The hypothesis to explain this results is related to the previous one considering lacunae as stress concentrators. If the concentration of these stress concentrators is too high close to the notch, the stress concentration state of the sample near this notch may increase more rapidly because of a higher density of stress concentrators, decreasing thus the energy needed to initiate the crack.

Considering fall like loading, there is also here a significant correlation between canal diameter and elastic toughness. As stated previously, it may imply that the initiation toughness is associated with the elasticity of the tissue. However, there is no correlation between the elastic toughness and the lacunar radius of curvature at this higher strain rate. As the loading is applied faster, the stress field may expand faster, and there might not be enough time for stress to concentrate sufficiently around the lacunae to relax the notch. We were able to predict the initiation toughness in the case of fall-like loading with better accuracy than under quasi-static loading, based on the lacunar density, the CX ratio, and the canal diameter.

Further, we can observe that the non-linear part of the deformation and the global toughness (J_{pl} and J , respectively) are both similarly correlated with structural and biochemical parameters (cf. Table 1 and Table 2). This is due to the fact that cortical bone crack propagation is mainly governed by these non-linear mechanisms, both under

quasi-static and fall-like loading. Furthermore, these non-linear mechanisms are more affected by the increase of the strain rate than the linear mechanisms^{24,26}. Therefore it is important to elucidate these mechanisms. From the results given in Table 1 we can observe that under quasi-static loading, the non-linear mechanisms of bone crack propagation are related to the canal diameter. Where the canals are larger, cracks have less difficulty to pass through the bone microstructure.

Relationships between the Haversian systems and the global toughness J have already been evidenced in a previous study³³. It is well known that the osteons, which surround the vascular canals, play a major role in crack propagation mechanisms. When a crack encounters the interface between the interstitial tissue and the osteon, it can be arrested or deviated along this interface^{15,48,49}. This role as a barrier to crack propagation may come from the difference of elasticity between the osteon and its surrounding tissue^{20,50}. Illustration of these mechanisms can be seen in⁵¹, where SR μ CT was also used to image the samples. The hypothesis is thus that the correlation between bone toughness and the canal diameter is likely to be due to the influence of the osteon morphology on crack propagation, the morphology of the osteons being dependent on the morphology of the Haversian canals⁵². Furthermore, a previous study has shown that the pullout of the osteon from the interstitial tissue required less energy for larger osteons⁵³. The authors hypothesized that for larger canals, the shear stress at the cement line is larger relative to the tensile stress applied to the whole osteon, resulting in an easier debonding at the interface. This result is in accordance with the present study that state that cracks propagate more easily in a microstructure with larger canals.

We can also observe a significant relationship between the non-linear toughness and the radius of curvature of the lacunae. To the authors' knowledge, there is no data about this in the literature. It is however known that the lacunae can guide the cracks during propagation^{47,54}. This is in accordance with the previously mentioned hypothesis that osteocyte lacunae act as stress concentrators. Christen et al. also hypothesized that the stress concentration near the lacunae may involve a blunting of the crack, resulting in increased toughness⁴⁷. This supports the results found here and highlights the stress concentrators, and thus energy dissipating, role played by osteocyte lacunae during crack propagation under quasi-static loading.

Finally we found that the CX ratio improves the estimation of the toughness, both the plastic and the global, in a multi variate model. We have shown in a previous study that the maturation of the enzymatic cross-links may have a minor influence on human cortical bone toughness²⁶. The present results support this minor effect. The associated mechanisms may be the interfibrillar sliding that consumes energy during loading^{12,55}. With a higher CX ratio, the tissue contains more immature cross-links relative to mature cross-links. As these mature cross-links are divalent compared to the trivalent mature cross-links, they may need less energy to break and thus encourage this interfibrillar sliding mechanism.

Under fall-like loading, we found no significant correlation between the non-linear toughness and structural or compositional features. This suggests that in the case of a fall, the mechanisms described above are much less efficient. Because of the higher loading

rate, the microstructure's response to crack propagation may not be the same, for example because of the time dependent nature of some bone features. It is known that at higher loading rate, there is a stiffening of bone tissue⁵⁶. In a previous study, based on the "He and Hutchinson framework", Zimmerman et al. hypothesized that the stiffening of the tissue may change the osteons deflection capacity^{20,50}. This stiffening of the tissue may also modify the strain concentration effect around the osteocyte lacunae, resulting in a straighter crack propagation path.

Regarding the correlations results, the linear regressions (Table 1) obtained in the current study may appear quite low compare to other studies investigating the relationships between cortical bone biomechanical properties and biochemical or structural properties ($\rho_{\text{Spearman}} = 0.66$ in the current study, $r = 0.78$ in⁵⁷, $r = 0.73$ in⁵⁸, $r = 0.94$ in⁵⁹). In most of the studies, the biomechanical parameter investigated was bone strength (MPa) using continuum mechanics, whereas in the current study the investigated parameters is the toughness (MPa.m^{0.5}) and more particularly the associated strain energy release rate²⁴, are related to the fracture mechanics field. Strength and toughness are two mechanical parameters that provide information on the ultimate mechanical properties of the studied materials. Nevertheless, they do not give the same information and it has been shown that bone strength is poorly correlated to the global toughness (J)⁶⁰. Strength is the mechanical stress at which the deformation of the material becomes non-recoverable⁶¹. The toughness of bone tissue gives information on the mechanical energy that is needed to initiate and propagate a crack from a pre-existing defect^{45,46,62,63}). This results in a parameter that is dependent on a local area surrounding the notch. Some previous works already studied the correlation coefficient between bone toughness and bone parameters. For instance, a low R^2 between bone toughness and the degree of mineralisation has been measured for the elastic toughness ($\rho_{\text{Spearman}} = 0.29$ in⁶⁴) and as non-significant when dealing with the global toughness^{33,64} whereas the correlation is significant between bone strength and mineralisation⁵⁷⁻⁵⁹. The toughness of bone might be more sensitive to the structure heterogeneities observable in cortical bone tissue^{65,66}. This is why the authors investigated the relationships between bone toughness and bone cortical structure at a lower length scale, such as the lacunar scale.

The main limitations of this study are related to the population investigated. The population used for the assessment of bone mechanical and structural properties comprised only 8 donors, which is a relatively small effective population. The main reasons for the limited sample size is the limited access to image acquisition time at synchrotron facilities, and the very large data sets that this modality yields. Despite of this, it can be seen that the population offers a large variety of mechanical, structural and compositional properties²⁴⁻²⁶. This somewhat alleviates the potential problem of a small population size. The wide range of properties still allowed the differences in structural and compositional properties to explain the differences in mechanical properties. Further, the population is not representative of the general population, in terms of gender and age. We investigated a population of aged female (50 y.o. to 91 y.o.) donors. It is known, however, that the population of post-menopausal women is more at risk of bone fracture^{67,68}. It is thus relevant to assess bone fracture properties on such a population. The results obtained here show that, in order to improve our biomechanical knowledge on bone fracture, it is relevant to investigate bone mechanical properties at rates that are

representative of the reality of falls. It is clear that bone fracture mechanisms are highly dependent on the loading rate. While these mechanisms are widely studied and well known under standard, quasi-static loading, there is still a substantial lack of data regarding higher loading rates. Therefore, the development of mechanical models of bone under realistic solicitation due to a fall, both considering loading rate and loading direction, represents a real challenge and will be highly useful for the improvement of prediction and prevention of bone fracture.

Conclusion

In this study, we have investigated the relationships between cortical bone toughness and its structural and compositional properties considering two loading conditions, representing walking and falls. Significant influence of the structure and composition on the initiation toughness was found in the two loading conditions. However, while the propagation of the crack is influenced by microstructural and compositional features under quasi-static loading, these features have less importance in the case of a fall. Further, since non-linear crack propagation mechanisms account for a large part of the global toughness, it will be important to study why an increase of the loading rate has a drastic effect on them.

Acknowledgements

The authors want to thank Cécile Olivier, Evelyne Gineyts, Leila Benboubaker and Pierre-Jean Gouttenoire for their technical support. The authors acknowledge the ESRF ID19 staff for its support for synchrotron data acquisition during the experiment MD923. This work was supported by the LabEx PRIMES (ANR-11-LABX-0063) within the program "Investissements d'Avenir" (ANR-11-IDEX-0007). This study was also partly funded by the Région Auvergne-Rhône-Alpes (14-011125-01) and by the ANR project MULTIPS (ANR-13-BS09-0006).

References

1. Siris ES, Chen Y-T, Abbott T a, et al. Bone mineral density thresholds for pharmacological intervention to prevent fractures. *Arch Intern Med* 2004; 164: 1108–1112.
2. Siris ES, Adler R, Bilezikian J, et al. The clinical diagnosis of osteoporosis: A position statement from the National Bone Health Alliance Working Group. *Osteoporos Int* 2014; 25: 1439–1443.
3. Johnell O, Kanis J a. An estimate of the worldwide prevalence, mortality and disability associated with hip fracture. *Osteoporos Int* 2006; 15: 897–902.
4. Genant HK, Engelke K, Fuerst T, et al. Noninvasive assessment of bone mineral and structure: state of the art. *J Bone Miner Res* 1996; 11: 707–730.
5. Wachter NJ, Augat P, Krischak GD, et al. Prediction of cortical bone porosity in vitro by microcomputed tomography. *Calcif Tissue Int* 2001; 68: 38–42.
6. van Rietbergen B, Ito K. A survey of micro-finite element analysis for clinical assessment of bone strength: The first decade. *J Biomech* 2015; 48: 832–841.

7. Seeman E, Delmas PD. Bone quality--the material and structural basis of bone strength and fragility. *N Engl J Med* 2006; 354: 2250–2261.
8. Yeni YN, Brown CU, Gruen T a., et al. The relationships between femoral cortex geometry and tissue mechanical properties. *J Mech Behav Biomed Mater* 2013; 21: 9–16.
9. Ritchie RO. Mechanisms of fatigue crack propagation in metals, ceramics and composites: Role of crack tip shielding. *Mater Sci Eng A* 1988; 103: 15–28.
10. Nalla RK, Kruzic JJ, Ritchie RO. On the origin of the toughness of mineralized tissue: Microcracking or crack bridging? *Bone* 2004; 34: 790–798.
11. Zimmermann EA, Schaible E, Bale H, et al. Age-related changes in the plasticity and toughness of human cortical bone at multiple length scales. *Proc Natl Acad Sci* 2011; 108: 14416–14421.
12. Gupta HS, Krauss S, Kerschnitzki M, et al. Intrafibrillar plasticity through mineral/collagen sliding is the dominant mechanism for the extreme toughness of antler bone. *J Mech Behav Biomed Mater* 2013; 28: 366–382.
13. Tang SY, Vashishth D. Non-enzymatic glycation alters microdamage formation in human cancellous bone. *Bone* 2010; 46: 148–154.
14. Zioupos P, Hansen U, Currey JD. Microcracking damage and the fracture process in relation to strain rate in human cortical bone tensile failure. *J Biomech* 2008; 41: 2932–2939.
15. O'Brien FJ, Taylor D, Lee TC. The effect of bone microstructure on the initiation and growth of microcracks. *J Orthop Res* 2005; 23: 475–480.
16. Burr DB, Schaffler MB, Frederickson RG. Composition of the cement line and its possible mechanical role as a local interface in human compact bone. *J Biomech* 1988; 21: 939–945.
17. Koester KJ, Ager JW, Ritchie RO. The true toughness of human cortical bone measured with realistically short cracks. *Nat Mater* 2008; 7: 672–677.
18. Berteau J-P, Gineyts E, Pithioux M, et al. Ratio between mature and immature enzymatic cross-links correlates with post-yield cortical bone behavior: An insight into greenstick fractures of the child fibula. *Bone* 2015; 79: 190–195.
19. Depalle B, Qin Z, Shefelbine SJ, et al. Influence of cross-link structure, density and mechanical properties in the mesoscale deformation mechanisms of collagen fibrils. *J Mech Behav Biomed Mater* 2015; 52: 1–13.
20. Zimmermann EA, Gludovatz B, Schaible E, et al. Fracture resistance of human cortical bone across multiple length-scales at physiological strain rates. *Biomaterials* 2014; 35: 5472–5481.
21. Ural A, Zioupos P, Buchanan D, et al. The effect of strain rate on fracture toughness of human cortical bone: A finite element study. *J Mech Behav Biomed Mater* 2011; 4: 1021–1032.
22. Kulin RM, Jiang F, Vecchio KS. Loading rate effects on the R-curve behavior of cortical bone. *Acta Biomater* 2011; 7: 724–732.
23. Tinetti ME. Preventing falls in elderly persons. *N Engl J Med* 2003; 348: 42–49.
24. Gauthier R, Follet H, Langer M, et al. Strain rate influence on human cortical bone toughness: A comparative study of four paired anatomical sites. *J Mech Behav Biomed Mater* 2017; 71: 223–230.
25. Gauthier R, Langer M, Follet H, et al. 3D micro structural analysis of human

- cortical bone in paired femoral diaphysis, femoral neck and radial diaphysis. *J Struct Biol* 2018; 204: 182–190.
26. Gauthier R, Follet H, Langer M, et al. Relationships between human cortical bone toughness and collagen cross-links on paired anatomical locations. *Bone* 2018; 112: 202–211.
 27. Foldhazy Z. Exercise-induced strain and strain rate in the distal radius. *J Bone Jt Surg - Br Vol* 2005; 87-B: 261–266.
 28. American Society for Testing and Materials. Standard Test Method for Linear-Elastic Plane-Strain Fracture Toughness of Metallic Materials. *Annu B ASTM Stand* 1997; 03: E 399 – 90.
 29. Irwin GR. Analysis of stresses and strains near the end of cracking traversing a plate. *J Appl Mech* 1957; 24: 361–364.
 30. Dong P, Hauptert S, Hesse B, et al. 3D osteocyte lacunar morphometric properties and distributions in human femoral cortical bone using synchrotron radiation micro-CT images. *Bone* 2014; 60: 172–185.
 31. Rho JY, Kuhn-Spearing L, Zioupos P. Mechanical properties and the hierarchical structure of bone. *Med Eng Phys* 1998; 20: 92–102.
 32. Yeni YN, Brown CU, Wang Z, et al. The influence of bone morphology on fracture toughness of the human femur and tibia. *Bone* 1997; 21: 453–459.
 33. Granke M, Makowski AJ, Uppuganti S, et al. Prevalent role of porosity and osteonal area over mineralization heterogeneity in the fracture toughness of human cortical bone. *J Biomech* 2016; 49: 2748–2755.
 34. Tang SY, Vashishth D. The relative contributions of non-enzymatic glycation and cortical porosity on the fracture toughness of aging bone. *J Biomech* 2011; 44: 330–336.
 35. Wachter N., Krischak G., Mentzel M, et al. Correlation of bone mineral density with strength and microstructural parameters of cortical bone in vitro. *Bone* 2002; 31: 90–95.
 36. Nair AK, Gautieri A, Chang S-W, et al. Molecular mechanics of mineralized collagen fibrils in bone. *Nat Commun* 2013; 4: 1724.
 37. Gupta HS, Seto J, Wagermaier W, et al. Cooperative deformation of mineral and collagen in bone at the nanoscale. *Proc Natl Acad Sci U S A* 2006; 103: 17741–17746.
 38. Granke M, Grimal Q, Saïed A, et al. Change in porosity is the major determinant of the variation of cortical bone elasticity at the millimeter scale in aged women. *Bone* 2011; 49: 1020–1026.
 39. Parnell WJ, Grimal Q. The influence of mesoscale porosity on cortical bone anisotropy. Investigations via asymptotic homogenization. *J R Soc Interface* 2009; 6: 97–109.
 40. Bala Y, Lefevre E, Roux JP, et al. Pore network microarchitecture influences human cortical bone elasticity during growth and aging. *J Mech Behav Biomed Mater* 2016; 63: 164–173.
 41. Rath Bonivtch A, Bonewald LF, Nicoletta DP. Tissue strain amplification at the osteocyte lacuna: A microstructural finite element analysis. *J Biomech* 2007; 40: 2199–2206.
 42. Verbruggen SW, Vaughan TJ, McNamara LM. Strain amplification in bone

- mechanobiology: a computational investigation of the in vivo mechanics of osteocytes. *J R Soc Interface* 2012; 9: 2735–2744.
43. Varga P, Hesse B, Langer M, et al. Synchrotron X-ray phase nano-tomography-based analysis of the lacunar-canalicular network morphology and its relation to the strains experienced by osteocytes in situ as predicted by case-specific finite element analysis. *Biomech Model Mechanobiol*. Epub ahead of print 2014. DOI: 10.1007/s10237-014-0601-9.
 44. Nicoletta DP, Moravits DE, Gale AM, et al. Osteocyte lacunae tissue strain in cortical bone. *J Biomech* 2006; 39: 1735–1743.
 45. Griffith a. a. The Phenomena of Rupture and Flow in Solids. *Philos Trans R Soc A Math Phys Eng Sci* 1921; 221: 163–198.
 46. Inglis CE. Stresses in a plate due to the presence of cracks and sharp corners. *Trans. I.N.A.* 1913; XLIV: 15.
 47. Christen D, Levchuk A, Schori S, et al. Deformable image registration and 3D strain mapping for the quantitative assessment of cortical bone microdamage. *J Mech Behav Biomed Mater* 2012; 8: 184–193.
 48. Yeni YN, Norman TL. Calculation of porosity and osteonal cement line effects on the effective fracture toughness of cortical bone in longitudinal crack growth. *J Biomed Mater Res* 2000; 51: 504–509.
 49. Mischinski S, Ural A. Interaction of microstructure and microcrack growth in cortical bone: a finite element study. *Comput Methods Biomech Biomed Engin* 2011; 1–14.
 50. He M-Y, Hutchinson JW. Kinking of a Crack Out of an Interface. *J Appl Mech* 1989; 56: 270.
 51. Wolfram U, Schwiedrzik JJ, Mirzaali MJ, et al. Characterizing microcrack orientation distribution functions in osteonal bone samples. *J Microsc* 2016; 00: 1–14.
 52. Qiu S, Fyhrie DP, Palnitkar S, et al. Histomorphometric assessment of Haversian canal and osteocyte lacunae in different-sized osteons in human rib. *Anat Rec - Part A Discov Mol Cell Evol Biol* 2003; 272: 520–525.
 53. van Oers RFM, Ruimerman R, van Rietbergen B, et al. Relating osteon diameter to strain. *Bone* 2008; 43: 476–482.
 54. Voide R, Schneider P, Stauber M, et al. Time-lapsed assessment of microcrack initiation and propagation in murine cortical bone at submicrometer resolution. *Bone* 2009; 45: 164–173.
 55. Hansma PK, Fantner GE, Kindt JH, et al. Sacrificial bonds in the interfibrillar matrix of bone. *J Musculoskelet Neuronal Interact* 2005; 5: 313–315.
 56. Hansen U, Zioupos P, Simpson R, et al. The effect of strain rate on the mechanical properties of human cortical bone. *J Biomech Eng* 2008; 130: 011011.
 57. Louis O, Boulpaep F, Willnecker J, et al. Cortical mineral content of the radius assessed by peripheral QCT predicts compressive strength on biomechanical testing. *Bone* 1995; 16: 375–379.
 58. Hsu JT, Wang SP, Huang HL, et al. The assessment of trabecular bone parameters and cortical bone strength: A comparison of micro-CT and dental cone-beam CT. *J Biomech* 2013; 46: 2611–2618.
 59. Zysset PK, Dall'ara E, Varga P, et al. Finite element analysis for prediction of

- bone strength. *Bonekey Rep* 2013; 2: 386.
60. Zioupos P, Kaffy C, Currey JD. Tissue heterogeneity, composite architecture and fractal dimension effects in the fracture of ageing human bone. *Int J Fract* 2006; 139: 407–424.
 61. Ritchie RO. The conflicts between strength and toughness. *Nat Mater* 2011; 10: 817–822.
 62. Rice JR, Rosengren GF. Plane strain deformation near a crack tip in a power-law hardening material. *J Mech Phys Solids* 1968; 16: 1–12.
 63. Nalla RK, Stölken JS, Kinney JH, et al. Fracture in human cortical bone: Local fracture criteria and toughening mechanisms. *J Biomech* 2005; 38: 1517–1525.
 64. Granke M, Makowski AJ, Uppuganti S, et al. Identifying Novel Clinical Surrogates to Assess Human Bone Fracture Toughness. *J Bone Miner Res* 2015; 30: 1290–1300.
 65. Zimmermann EA, Ritchie RO. Bone as a Structural Material. *Adv Healthc Mater* 2015; 4: 1287–1304.
 66. McCormack J, Stover SM, Gibeling JC, et al. Effects of mineral content on the fracture properties of equine cortical bone in double-notched beams. *Bone* 2012; 50: 1275–1280.
 67. Kimmel DB, Recker RR, Gallagher JC, et al. A comparison of iliac bone histomorphometric data in post-menopausal osteoporotic and normal subjects. *Bone Miner* 1990; 11: 217–235.
 68. Court-Brown CM, Caesar B. Epidemiology of adult fractures: A review. *Injury* 2006; 37: 691–697.